

Triangular Plate Bending Elements with Enforced Compatibility

J. W. HARVEY*

AiResearch Manufacturing Company, Phoenix, Ariz.

AND

S. KELSEY†

University of Notre Dame, Notre Dame, Ind.

A technique for establishing complete normal slope compatibility at the interfaces of triangular plate bending elements is presented. The nodal connections result in a deficiency of one parameter per common boundary for providing automatic conformity. Each deficiency is compensated by a constraint, imposed by the Lagrange multiplier method, which forces compatibility at the midside. The element displacement is described by a complete cubic interpolation polynomial. Nodal freedoms are the displacement w , slopes w_x , w_y at each corner and w at the centroid. Derivation of the stiffness and other matrices required for the basic element is straightforward. Results presented, including deflections, critical loads and vibration frequencies are in general more accurate than from other available elements of equivalent complexity.

Nomenclature

a_1	= $x_3 - x_2$, etc. (Fig. 1)
b_1	= $y_2 - y_3$, etc. (Fig. 1)
B_x, B_y	= transformation matrices [Eqs. (2), (3), and Appendix]
C, C_{jk}	= constraint matrices [Eqs. (13) and (14)]
D	= plate bending stiffness = $Et^3/12(1 - \nu^2)$
G	= numerical matrix [Eq. (8) and Appendix]
k, K	= stiffness matrices of element and element assemblage, respectively
\bar{M}	= numerical matrix [Eq. (9) and Appendix]
p	= pressure on plate
r, R	= vectors of nodal displacements and forces, defined for complete assemblage
t	= plate thickness
T	= transformation matrix [Eq. (5) and Appendix]
w	= transverse displacement
w_x	= $\partial w / \partial x$
x, y	= Cartesian coordinates, origin at triangle centroid 0
0, 1, 2, 3	= nodal point numbers
λ	= vector of Lagrange multipliers [Eq. (15)]
ν	= Poisson's ratio
ρ	= nodal displacement vector for element
$\sigma_{xx}, \sigma_{yy}, \sigma_{xy}$	= membrane direct and shear stresses
Ω	= area of triangle = $\frac{1}{2}(a_3b_2 - a_2b_3)$, etc.

I. Introduction

IN the design of deformation modes for finite elements it is generally accepted that the kinematic compatibility conditions are satisfied implicitly by the definition of the problem in terms of displacement unknowns. Modes are therefore sought which automatically guarantee complete compatibility on the inter-element boundaries by the matching of common nodal freedoms. Any deficiencies in this respect are either accepted, and the element described as nonconforming, or eliminated by modification of the polynomials which form the deformation functions. The modification usually consists of a constraint on the boundary deformation of the element, compensated by greater freedom elsewhere to maintain the requisite degrees of freedom.

Presented as Paper 70-136 at the AIAA 8th Aerospace Sciences Meeting, New York, January 19-21, 1970; submitted February 19, 1970; revision received July 20, 1970.

* Engineering Specialist, Engineering Mechanics Division.

† Professor, Department of Civil Engineering. Member AIAA.

For the triangular bending element, with only three freedoms (w, w_x, w_y) specified at each corner, the constraint necessary to ensure complete compatibility consists in permitting only a linear variation of normal slope along each edge, while the displacement varies cubically. In conforming elements so constructed, the compensating freedom has been provided by using separate (though compatible) cubic polynomials within subdivisions of the triangle^{1,2} or by augmenting the basic single cubic with higher order polynomial terms.^{3,4}

The present paper describes an alternative approach to producing conformity which has been found simple and useful.⁷ Instead of modifying the individual element displacement functions so as to yield a simplified boundary deformation, the basic nonconforming behavior is initially accepted. Incompatibility is eliminated by an explicit constraint condition imposed on both elements meeting at an edge. Since the constraints on different edges must be coupled through the elastic behavior of the element, this amounts to a system of constraints applied to the structure as a whole, which are enforced by the Lagrange multiplier technique.

The basic triangular element presented employs a complete cubic polynomial for the displacement function. Nodal freedoms are w, w_x, w_y at each corner and w at the triangle centroid. The quadratic variation of normal slope along each side requires, therefore, a single constraint equation for each side common to two triangles or at a clamped boundary of the plate. These equations are simple to form and assemble into the complete matrix, which describes the behavior of the assembled system of elements.

Because of the simplicity of the deformation modes, the derivation of elastic and geometric stiffness matrices as well as the consistent mass matrix is straightforward. The number of nodal freedoms may be reduced to nine by a statical condensation to eliminate the centroidal deflection. In this form, the basic element is equivalent to the T-10 element which was investigated, and discarded because of its excessive flexibility, by Clough and Tocher in Ref. 1. Results presented here demonstrate that with enforced slope compatibility between elements, it is capable of yielding very satisfactory accuracy.

II. Basic Element Matrices

The geometry of the element is described with reference to a Cartesian axis system, Oxy , parallel to the global axes used

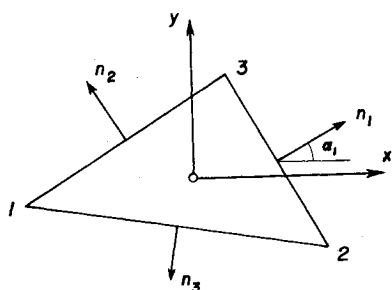


Fig. 1 Geometry of triangular element.

and with origin at the triangle centroid (Fig. 1). Midpoints of the sides are numbered for reference, but do not constitute element nodes in the usual sense. Directions n_1, n_2, n_3 , are the outward normals to the sides shown.

The deformation modes obtained by matching a complete cubic polynomial to the nodal displacement vector,

$$\rho = \{w_0 w_1 w_2 w_3 w_4 w_5 w_6 w_7 w_8 w_9\} \quad (1)$$

have been discussed by Felippa⁶ in connection with a plane stress element with quadratically varying strain and need not be repeated here.

From the deformation functions, it is straightforward to establish the two (6×10) matrices, $\mathbf{B}_x, \mathbf{B}_y$, and the (9×10) matrix, \mathbf{T} , which give the slopes and curvatures at the reference points in terms of nodal displacements.

Thus,

$$\theta_x = \{w_{x1} w_{x2} w_{x3} w_{x4} w_{x5} w_{x6}\} = \mathbf{B}_x \rho \quad (2)$$

$$\theta_y = \{w_{y1} w_{y2} w_{y3} w_{y4} w_{y5} w_{y6}\} = \mathbf{B}_y \rho \quad (3)$$

$$\phi_i = \{w_{xxi} w_{yyi} 2w_{xyi}\} \quad i = 1, 2, 3 \quad (4)$$

$$\phi = \{\phi_1 \phi_2 \phi_3\} = \mathbf{T} \rho \quad (5)$$

θ_x, θ_y, ϕ define completely the slope and curvature variation over the triangle. $\mathbf{B}_x, \mathbf{B}_y, \mathbf{T}$ are displayed in the Appendix.

With linear variation of curvatures between the nodal values, and the assumption of constant thickness, the stiffness matrix, corresponding to the nodal displacement vector ρ , is given by standard theory as

$$\mathbf{k} = \mathbf{T}^T \begin{bmatrix} 2E & E & E \\ E & 2E & E \\ E & E & 2E \end{bmatrix} \mathbf{T} \quad (6)$$

where, for an isotropic plate,

$$E = (D\Omega/12) \begin{bmatrix} 1 & \nu & 0 \\ \nu & 1 & 0 \\ 0 & 0 & (1-\nu)/2 \end{bmatrix} \quad (7)$$

Matrices $\mathbf{B}_x, \mathbf{B}_y$, besides being needed for the formation of the constraint equations, are basic data for the geometric stiffness \mathbf{k}_G , due to membrane stresses $\sigma_{xx}, \sigma_{yy}, \sigma_{xy}$. For uniform membrane stresses over the element, we find

$$\mathbf{k}_G = t\sigma_{xx}\mathbf{B}_x^T\mathbf{G}\mathbf{B}_x + t\sigma_{yy}[\mathbf{B}_x^T\mathbf{G}\mathbf{B}_y + \mathbf{B}_y^T\mathbf{G}\mathbf{B}_x] + t\sigma_{xy}\mathbf{B}_y^T\mathbf{G}\mathbf{B}_y \quad (8)$$

The (6×6) numerical matrix \mathbf{G} is shown in the Appendix, as is the (10×10) $\bar{\mathbf{M}}$ which provides the consistent mass matrix \mathbf{M} , i.e.,

$$\mathbf{M} = \mu \mathbf{A}^T \bar{\mathbf{M}} \mathbf{A} \quad (9)$$

where μ is the mass per unit area of the plate, and \mathbf{A} is the (10×10) matrix displayed in the Appendix.

$\bar{\mathbf{M}}$ also serves for the calculation of kinematically consistent forces \mathbf{P} at the element nodes. If the pressure distribution is described by a vector,

$$\mathbf{p} = \{p_0 p_1 p_2 p_3 p_4 p_5 p_6 p_7 p_8 p_9\} \quad (10)$$

in the same way as the plate displacements in Eq. (1) we have

$$\mathbf{P} = \mathbf{A}^T \bar{\mathbf{M}} \mathbf{A} \mathbf{p} \quad (11)$$

III. Compatibility Constraints

The nodal connections of the elements result in a deficiency of one parameter per common boundary for automatic compatibility. This deficiency, as shown in Refs. 1 and 5, results in an excessively flexible assembly, where deflections converge to erroneous results with progressive grid refinement.

The deficiency noted previously stems from the normal slopes $(\partial w / \partial n)$ at matching element edges being described by a quadratic function, requiring three parameters, whereas the nodal connections at the common edge provide only two. If, however, the slopes are forced to match at some intermediate point (for convenience, the midpoint is chosen), then continuity of slope will be established all along the edge. This condition is enforced by the method of constraints as follows.

The normal slope at the center of side 2-3 (Fig. 1) is

$$w_n = w_{x4} \cos \alpha_1 + w_{y4} \sin \alpha_1 = -(1/l_1)(a_1 \mathbf{B}_{x4} + b_1 \mathbf{B}_{y4}) \rho \quad (12)$$

where

$$a_1 = x_3 - x_2, b_1 = y_2 - y_3, l_1 = (a_1^2 + b_1^2)^{1/2}$$

$\mathbf{B}_{x4}, \mathbf{B}_{y4}$ are the fourth rows of $\mathbf{B}_x, \mathbf{B}_y$, respectively.

The condition for continuity of normal slope at a typical edge between two elements k and l may thus be written

$$\mathbf{C}_{jk} \rho_k + \mathbf{C}_{jl} \rho_l = 0 \quad (13)$$

$\mathbf{C}_{jk}, \mathbf{C}_{jl}$ are (1×10) matrices of the type

$$[a_1 \mathbf{B}_{x4} + b_1 \mathbf{B}_{y4}]$$

the suffixes being determined by the side of the triangle involved. Suffix j refers to the number of the common edge (or clamped edge) in a global numbering system of the constraints. Since ρ_i and ρ_k are subvectors of the master displacement vector \mathbf{r} , the complete set of constraint equations may be assembled into a matrix form, i.e.,

$$\mathbf{C} \mathbf{r} = 0 \quad (14)$$

Using a Lagrange multiplier technique to enforce constraint conditions, while simultaneously satisfying the equilibrium equations defined by stiffness matrix \mathbf{K} , leads to the partitioned equation

$$\begin{bmatrix} \mathbf{K} & \mathbf{C}^T \\ \mathbf{C} & \mathbf{0} \end{bmatrix} \begin{bmatrix} \mathbf{r} \\ \lambda \end{bmatrix} = \begin{bmatrix} \mathbf{R} \\ \mathbf{0} \end{bmatrix} \quad (15)$$

The vector λ , of Lagrange multipliers, may be interpreted physically as generalized constraint forces necessary to remove the slope mismatches from the loaded plate.

In Ref. 9, Jones has proposed an extensive use of Lagrangian multipliers, in conjunction with the Reissner variational principle, to generalize the finite-element method. Though not derived in this way, the present approach may be regarded as a special case of Jones' generalization. A recent paper by Tong¹⁰ also gives a more general theory, of

Table 1 Central deflection of simply supported square plate under uniform pressure \sim values of $10^5 D w_c / p L^4$

N	HCT	$LCCT-12$	$Q-19$	$BCIZ$	P	$T10$
2	355	400	402	428	410	873
3	416	407	857
4	393	405	406	412	406	849

Exact value = 406.

Table 2 Central deflection of simply supported square plate under central load $W \sim$ values of $10^6 D w_c / W L^2$

N	HCT	$LCCT-12$	$Q-19$	$BCIZ$	P
2	1050	1125	1110	1174	1094
3	1166	1131
4	1122	1155	1155	1165	1158

Exact value = 1160.

which the present work may be viewed as a particular example.

IV. Solution of the Equations

The coefficient matrix in Eq. (15) is of course appreciably larger than the stiffness matrix corresponding to displacements specified at the nodal points alone. For a large system, with n nodal points, upper bounds to the number of rows in \mathbf{K} and \mathbf{C} are $5n$ and $3n$, respectively. The $2n$ displacements (w_0) at the triangle centroids may be eliminated by statical condensation of the individual element stiffness matrices, though this complicates the storage or regeneration of the basic element matrices when element geometry is not uniform.

To retain a banded structure for the matrix, the \mathbf{r} and λ variables may be intermingled, giving a matrix structure similar to that obtained if midside slopes are used as explicit kinematic variables as with the $LCCT-12$ elements described in Ref. 2. The resulting band width is greater than for the \mathbf{K} alone.

In the numerical solution, it is important to scale the constraint equations and variables, so that the elements of \mathbf{C} and \mathbf{K} have the same order of magnitude. Given proper scaling, however, and with a Gauss elimination method of solution which uses pivoting, it is found that Eq. (15) is slightly better conditioned than the unconstrained stiffness equation. Thus, the additional equations actually result in an enhanced numerical accuracy.

V. Numerical Applications

The simply supported square plate, of which a quarter is shown in Fig. 2, has been analyzed for static loads (Tables 1 and 2), vibration frequency (Table 3), and critical stress under biaxial compression. Results for other elements from Refs. 1-3 and 8 are included for comparison and are identified by the following abbreviations: HCT = conforming triangular element of Ref. 1; $LCCT-12$ = conforming triangular element of Ref. 2 (employing midside slopes as additional displacement variables); $Q-19$ = conforming quadrilateral elements of Ref. 2; $BCIZ$ = nonconforming triangular element of Ref. 3; $T10$ = present element without constraint; and P = present element with constraint.

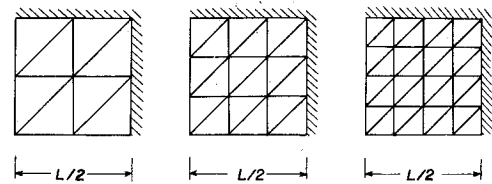
The $T10$ results are included in Table 1 to demonstrate the excessive flexibility of the unconstrained elements, the notation, $T10$, being taken from Ref. 1.

Uniform Load

Table 1 shows the central deflection w_c of the uniformly loaded plate. Some caution is necessary in making comparisons, since only the analyses for P , $T10$ and $BCIZ$ use

Table 3 Percentage error in fundamental vibration frequency of simply supported square plate

N	HCT	$Q-9$	$BCIZ$	P
2	2.8	1.5	-3.3	0.4
3	1.2	...	-1.7	0.2
4	0.7	0.4	-1.1	0.1

**Fig. 2 Grid patterns for square plate, shown for upper right quarter plate.**

kinematically consistent nodal forces. Also, the results for HCT , taken from Ref. 1, are based on the grid patterns of Fig. 2 for the top left quarter of the plate. For $Q-19$ and $LCCT-12$, the figures are taken from the charts of Ref. 2.

Concentrated Load at Center

Table 2 compares the central deflection under a central point load for the different elements. Here, the load representations are identical and comparisons are correspondingly more meaningful. The deflections also give a direct measure of the strain energy of the loaded plate.

Natural Frequency

Percentage errors in the values of the fundamental vibration frequency, based on different elements, are presented in Table 3. Consistent mass matrices were used in all cases.

Buckling Stress

For uniform biaxial compression of the square, simply supported plate, percentage errors in the critical value of the stress are shown in Table 4 for the present element with constraints and for the $BCIZ$ element. The usual method of calculating critical stress, by iterative or other classical eigenvalue analysis, was avoided in this problem by means of a Southwell plot technique.

VI. Conclusions

A constraint technique for establishing normal slope compatibility between triangular plate bending element has been presented. The simplicity of formulation and the accuracy of results obtainable with a basically nonconforming element so constrained has been demonstrated.

The constraint formulation results in a coefficient matrix larger and wider banded than if nodal connections alone are used. However, the enlargement of the coefficient matrix does not cause any deterioration of the conditioning of the system.

Applications of the technique to other plate bending elements, as well as to plane stress and shell elements, has been demonstrated elsewhere.⁷ The method may also be extended to impose equilibrium-type constraint conditions.

Appendix: Basic Matrices for Elements

$$\mathbf{G} = \frac{\Omega}{180} \begin{bmatrix} 6 & -1 & -1 & -4 & 0 & 0 \\ -1 & 6 & -1 & 0 & -4 & 0 \\ -1 & -1 & 6 & 0 & 0 & -4 \\ -4 & 0 & 0 & 32 & 16 & 16 \\ 0 & -4 & 0 & 16 & 32 & 16 \\ 0 & 0 & -4 & 16 & 16 & 32 \end{bmatrix}$$

Table 4 Percentage error in critical stress for square simply supported plate under biaxial compression

N	2	3	4
P	1.09	0.28	0.05
$BCIZ$	2.67	1.56	1.09

$$\mathbf{M} = \frac{\Omega}{5040} \begin{bmatrix} 180 & 9 & 9 & 30 & 30 & 3 & 12 & 12 & 3 & 6 \\ 9 & 180 & 9 & 12 & 3 & 30 & 30 & 3 & 12 & 6 \\ 9 & 9 & 180 & 3 & 12 & 12 & 3 & 30 & 30 & 6 \\ 30 & 12 & 3 & 12 & 6 & 3 & 9 & 3 & 2 & 3 \\ 30 & 3 & 12 & 6 & 12 & 2 & 3 & 9 & 3 & 3 \\ 3 & 30 & 12 & 3 & 2 & 12 & 6 & 3 & 9 & 3 \\ 12 & 30 & 3 & 9 & 3 & 6 & 12 & 2 & 3 & 3 \\ 12 & 3 & 30 & 3 & 9 & 3 & 2 & 12 & 6 & 3 \\ 3 & 12 & 30 & 2 & 3 & 9 & 3 & 6 & 12 & 3 \\ 6 & 6 & 6 & 3 & 3 & 3 & 3 & 3 & 3 & 2 \end{bmatrix}$$

$$\mathbf{A} = \begin{bmatrix} 1 & & & & & & & & & \\ & & & 1 & & & & & & \\ & & & & & & 1 & & & \\ & 3 & & a_3 & -b_3 & & & & & \\ & 3 & & -a_2 & b_2 & & & & & \\ & & & & & 3 & & a_1 & -b_1 & \\ & & & & & 3 & & -a_3 & b_3 & \\ & & & & & & 3 & & a_2 & -b_2 \\ & & & & & & & 3 & -a_1 & b_1 \\ 27 & -7 & 3x_1 & 3y_1 & -7 & 3x_2 & 3y_2 & -7 & 3x_3 & 3y_3 \end{bmatrix}$$

$$\mathbf{B}_x = \frac{1}{8\Omega} \begin{bmatrix} & & 8\Omega & & & & & & & \\ & & & & & 8\Omega & & & & \\ & & & & & & & & 8\Omega & \\ 27b_1 & -7b_1 & 3x_1b_1 & 3y_1b_1 & 19y_3 - y_2 & a_1(4y_3 - y_2) & b_1(y_2 - 4y_3) & y_3 - 19y_2 & a_1(4y_2 - y_3) & b_1(y_3 - 4y_2) \\ 27b_2 & y_1 - 19y_3 & a_2(4y_3 - y_1) & b_2(y_1 - 4y_3) & -7b_2 & 3x_2b_2 & 3y_2b_2 & 19y_1 - y_3 & a_2(4y_1 - y_3) & b_2(y_3 - 4y_1) \\ 27b_3 & 19y_2 - y_1 & a_3(4y_2 - y_1) & b_3(y_1 - 4y_2) & y_2 - 19y_1 & a_3(4y_1 - y_2) & b_3(y_2 - 4y_1) & -7b_3 & 3x_3b_3 & 3y_3b_3 \end{bmatrix}$$

$$\mathbf{B}_y = \frac{1}{8\Omega} \begin{bmatrix} & & 8\Omega & & & & & & & \\ & & & & & 8\Omega & & & & \\ & & & & & & & & 8\Omega & \\ 27a_1 & -7a_1 & 3x_1a_1 & 3y_1a_1 & x_2 - 19x_3 & a_1(x_2 - 4x_3) & b_1(4x_3 - x_2) & 19x_2 - x_3 & a_1(x_3 - 4x_2) & b_1(4x_2 - x_3) \\ 27a_2 & 19x_3 - x_1 & a_2(x_1 - 4x_3) & b_2(4x_3 - x_1) & -7a_2 & 3x_2a_2 & 3y_2a_2 & x_3 - 19x_1 & a_2(x_3 - 4x_1) & b_2(4x_1 - x_3) \\ 27a_3 & x_1 - 19x_2 & a_3(x_1 - 4x_2) & b_3(4x_2 - x_1) & 19x_1 - x_2 & a_3(x_2 - 4x_1) & b_3(4x_1 - x_2) & -7a_3 & 3x_3a_3 & 3y_3a_3 \end{bmatrix}$$

References

¹ Clough, R. W. and Tocher, J. L., "Finite Element Stiffness Matrices for the Analysis of Plate Bending," *Proceedings of the Conference on Matrix Methods in Structural Mechanics*, Wright-Patterson Air Force Base, Ohio, 1965, pp. 515-545.

² Clough, R. W. and Felippa, C. A., "A Refined Quadrilateral Element for Analysis of Plate Bending," *Proceedings of the Second Conference on Matrix Methods in Structural Mechanics*, Wright-Patterson Air Force Base, Ohio, 1968, pp. 399-439.

³ Bazeley, G. P., Cheung, Y. K., Irons, B. M., and Zienkiewicz, O. C., "Triangular Elements in Plate Bending—Conforming and Nonconforming Solutions," *Proceedings of the Conference on Matrix Methods in Structural Mechanics*, Wright-Patterson Air Force Base, Ohio, 1965, pp. 547-576.

⁴ Irons, B. M., "A Conforming Quartic Triangular Element for Plate Bending," Computer Program Report, 1968, Centre for Numerical Methods in Engineering, Univ. of Wales, Swansea, Wales.

$$\mathbf{T} = \frac{1}{2\Omega^2} \begin{bmatrix} \mathbf{J}_1 & \mathbf{H}_{11} & \mathbf{H}_{12} & \mathbf{H}_{13} \\ \mathbf{J}_2 & \mathbf{H}_{21} & \mathbf{H}_{22} & \mathbf{H}_{23} \\ \mathbf{J}_3 & \mathbf{H}_{31} & \mathbf{H}_{32} & \mathbf{H}_{33} \end{bmatrix}$$

where

$$\mathbf{J}_1 = \{27b_2b_3 \quad 27a_2a_3 \quad 27A_{23}\}$$

$$\mathbf{H}_{11} = \begin{bmatrix} -3b_1^2 - 7b_2b_3 & 3x_1b_2b_3 + 4\Omega b_1 & 3y_1b_2b_3 \\ -3a_1^2 - 7a_2a_3 & 3x_1a_2a_3 & 3y_1a_2a_3 + 4\Omega a_1 \\ -6a_1b_1 - 7A_{23} & 4\Omega a_1 + 3x_1A_{23} & 4\Omega b_1 + 3y_1A_{23} \end{bmatrix}$$

$$\mathbf{H}_{12} = \begin{bmatrix} b_2(3b_2 - 7b_3) & 2b_2(a_3b_3 - \Omega) & -2b_2b_3^2 \\ a_2(3a_2 - 7a_3) & 2a_2a_3^2 & -2a_2(a_3b_3 + \Omega) \\ 6a_2b_2 - 7A_{23} & -2a_2a_3b_2 + 3x_2A_{23} & 2a_2b_2b_3 + 3y_2A_{23} \end{bmatrix}$$

$$\mathbf{H}_{13} = \begin{bmatrix} b_3(3b_3 - 7b_2) & -2b_3(a_2b_2 + \Omega) & 2b_3^2b_3 \\ a_3(3a_3 - 7a_2) & -2a_3^2a_3 & 2a_3(a_2b_2 - \Omega) \\ 6a_3b_3 - 7A_{23} & 2a_3a_3b_3 + 3x_3A_{23} & -2a_3b_3b_3 + 3y_3A_{23} \end{bmatrix}$$

$$A_{23} = a_2b_3 + a_3b_2$$

The remaining sub-matrices of \mathbf{T} are obtained by cyclic advance of all subscripts, e.g., \mathbf{H}_{13} yields \mathbf{H}_{21} by subscript changes: $3 \rightarrow 1, 2 \rightarrow 3$.

⁵ Clough, R. W., "The Finite Element Method in Structural Mechanics," *Stress Analysis*, edited by O. C. Zienkiewicz and O. C. Hollister, Wiley, New York, 1965.

⁶ Felippa, C. A., "Refined Finite Element Analysis of Linear and Nonlinear Two-Dimensional Structures," Rept. 66-22, 1966, Dept. of Civil Engineering, Univ. of California, Berkeley, Calif.

⁷ Harvey, J. W., "Constraint Technique in Finite Element Analysis," Ph.D. dissertation, Univ. of Notre Dame, Notre Dame, Ind. 1969.

⁸ Dickinson, S. M. and Henshell, R. N., "Clough-Tocher Triangular Plate Bending Element in Vibration," *AIAA Journal*, Vol. 7, No. 3, March 1969, pp. 560-561.

⁹ Jones, R. E., "A Generalization of the Direct-Stiffness Method of Structural Analysis," *AIAA Journal*, Vol. 2, No. 5, May 1964, pp. 821-826.

¹⁰ Tong, P., "New Displacement Hybrid Method for Solid Continua," *International Journal of Numerical Methods for Engineering*, Vol. II, 1970, pp. 73-83.